

# Imaging and spectroscopy at terahertz frequencies using hot electron bolometer technology\*

Eyal Gerecht<sup>\*\*a</sup>, Dazhen Gu<sup>a</sup>, Fernando Rodriguez-Morales<sup>b</sup>, and Sigfrid Yngvesson<sup>b</sup>

<sup>a</sup>National Institute of Standards and Technology, Boulder, CO 80305;

<sup>b</sup>Department of Electrical and Computer Engineering, University of Massachusetts at Amherst, MA 01003

## ABSTRACT

Imaging and spectroscopy at terahertz frequencies (defined roughly as 300 GHz – 3 THz) have great potential for both healthcare and homeland security applications. Terahertz frequencies correspond to energy level transitions of important molecules in biology and astrophysics. Terahertz radiation (T-rays) can penetrate clothing and, to some extent, can also penetrate biological materials, and because of their shorter wavelengths they offer higher spatial resolution than microwaves or millimeter waves.

We describe the development of a novel two-dimensional scanning, passive, terahertz imaging system based on a hot electron bolometer (HEB) detector element. HEB mixers are near quantum noise limited heterodyne detectors operating over the entire terahertz spectrum. HEB devices absorb terahertz radiation up to the visible range due to the very short momentum scattering times. The terahertz imaging system consists of a front-end heterodyne detector integrated with a state-of-the-art monolithic microwave integrated-circuit low-noise amplifier (MMIC LNA) on the same mixer block. The terahertz local oscillator (LO) signal is provided by a commercial harmonic multiplier source.

**Keywords:** terahertz imaging, terahertz spectroscopy, terahertz receivers, hot electron bolometers, heterodyne detectors, superconducting devices, quasi-optical systems, focal plane arrays.

## 1. INTRODUCTION

Terahertz radiation (T-rays) can penetrate clothes, dust, smoke, and biological materials better than infrared and visible light. This penetration capability and T-rays's shorter wavelengths have led to the development of imagers with higher spatial resolution compared with those based on microwaves or millimeter waves. Such applications include terahertz imagers for detecting concealed weapons, illicit drugs, and biological materials. Furthermore, the unique spectra of some materials in the terahertz spectrum have led to the development of ultra-sensitive spectrometers both for astrophysical and terrestrial applications.

Hot electron bolometric (HEB) mixer receivers for terahertz frequencies have been developed for the past ten years [1]. A few instruments based on HEB technology have been deployed or are ready for deployment for astrophysical applications [2,3,4,5]. In astronomical applications, observations of spectral lines have played a major role in expanding our understanding of the interstellar medium and planetary atmospheres. HEB mixers, which use nonlinear heating effects in superconductors near their transition temperature, have become an excellent candidate for applications requiring low noise temperatures at frequencies from 0.5 THz to 10 THz. The sensitivity of heterodyne receivers ('mixers') is usually expressed in terms of their double sideband (DSB) receiver noise temperature. Figure 1 illustrates the state-of-the-art DSB receiver noise tempera-

---

\*Work partly supported by the U.S. National Institute of Standards and Technology, not subject to U.S. copyright.

\*\*[gerecht@nist.gov](mailto:gerecht@nist.gov); phone (303) 497-4199; fax (303) 497-3970;

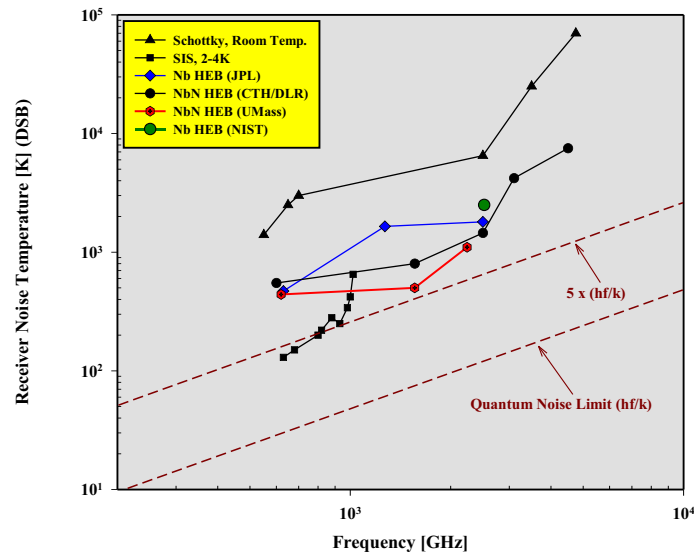


**Figure 1: Double-sideband receiver noise temperature for different heterodyne receivers over a wide frequency range.**

tures over a broad frequency range, for different types of terahertz receivers. The quantum noise limit for the DSB system noise temperature is  $hf/k$  (shown by the lower dashed line in Figure 1). The DSB receiver noise temperatures of the best receivers from 100 GHz to 2.5 THz approach the  $5 \times hf/k$  line (also shown by dashed line). Superconductor-insulator-superconductor (SIS) mixers have the best sensitivity up to and just above 1 THz, but are limited in frequency by the bandgap frequency of the superconductor material used for the SIS junction. The oldest technology, Schottky-barrier diodes (SBD), yields noise temperatures at terahertz frequencies that are at least an order of magnitude greater than those of hot electron bolometers. In order to achieve the required sensitivity for astronomical, remote-sensing, homeland security, and biomedical applications, we need to develop receivers operating at sensitivities near the quantum noise limit, plus focal plane arrays (FPAs) with multiple mixer elements. Moreover, the local oscillator (LO) power requirement of HEB mixers (a few hundred nanowatts) is about four orders of magnitude lower than that of Schottky barrier diode mixers. Maintaining a low LO power consumption is a major challenge in the development of multi-pixel focal plane arrays at terahertz frequencies. This is due to the difficulties encountered in producing sufficient LO power at terahertz frequencies.

The feasibility of a passive detection technique relies on the fact that all objects whose temperatures are above absolute zero (0 K) emit terahertz radiation. Their actual emission is related to the black-body radiation by a wavelength-dependent emissivity that is specific to the material in question. In other words, all objects behave like grey-body emitters with respect to the ideal black-body. By using ultra-sensitive HEB detectors, an imaging system can potentially distinguish between different materials in thermal equilibrium.

We present here results with a two-dimensional (2D) scanning terahertz passive heterodyne imaging system, currently under development [6]. The imager is based on a phonon-cooled quasi-optically coupled hot electron bolometric mixer integrated with an InP monolithic microwave integrated-circuit (MMIC) IF low-noise amplifier (LNA). A harmonic multiplier with an output power of about  $250 \mu\text{W}$  is employed as the local oscillator source, resulting in a very compact setup. Terahertz images are obtained by scanning the target with a flat mirror mounted on a computer-controlled elevation/azimuth translator. We chose 850 GHz as the operating frequency for our system, as it is one of the atmospheric windows for terahertz radiation and it gives relatively high spatial resolution. In principle, we could operate at any terahertz frequency.

## 2. TERAHERTZ IMAGER WITH HEB DETECTORS

Figure 2 shows a schematic diagram of a terahertz passive imager. The main components of such a system are the front-end detecting element, the local oscillator source, the optics design, and the data acquisition system. In order to produce a two-dimensional raster, the heterodyne receiver collects radiation from the scanned object through optical components, such as off-axis parabolic mirrors and a thin mylar beam-splitter, in both the elevation and azimuth directions. This signal beam is chopped against a room temperature black-body source. The intermediate frequency (IF) output signal is amplified by a cryogenic low-noise amplifier (LNA) cascaded with a back-end IF chain of tunable gain and bandwidth, operating at room temperature. The IF bandwidth of the receiver is limited by means of a band-pass filter, which is in turn connected to a standard microwave detector to produce a rectified voltage signal. This signal is then fed to a lock-in amplifier referenced by the chopping frequency. A dedicated data acquisition (DAQ) system collects the lock-in amplifier's output signal as a function of position with respect to the target. Next, we discuss the specific components of our terahertz passive imager.

### 2.1 HEB devices

HEBs are “surface” superconducting devices with extremely small parasitic reactances, even at the highest terahertz frequencies. The device is fabricated from an NbN film that has been sputtered onto a silicon substrate. The film thickness is typically 3.5 to 4 nm. A typical device size is 2  $\mu\text{m}$  (width) x 0.5  $\mu\text{m}$  (length). An HEB device integrated with a twin-slot antenna or a log-periodic self-complementary antenna is shown in Figure 3. The device can be matched to the antenna by changing its

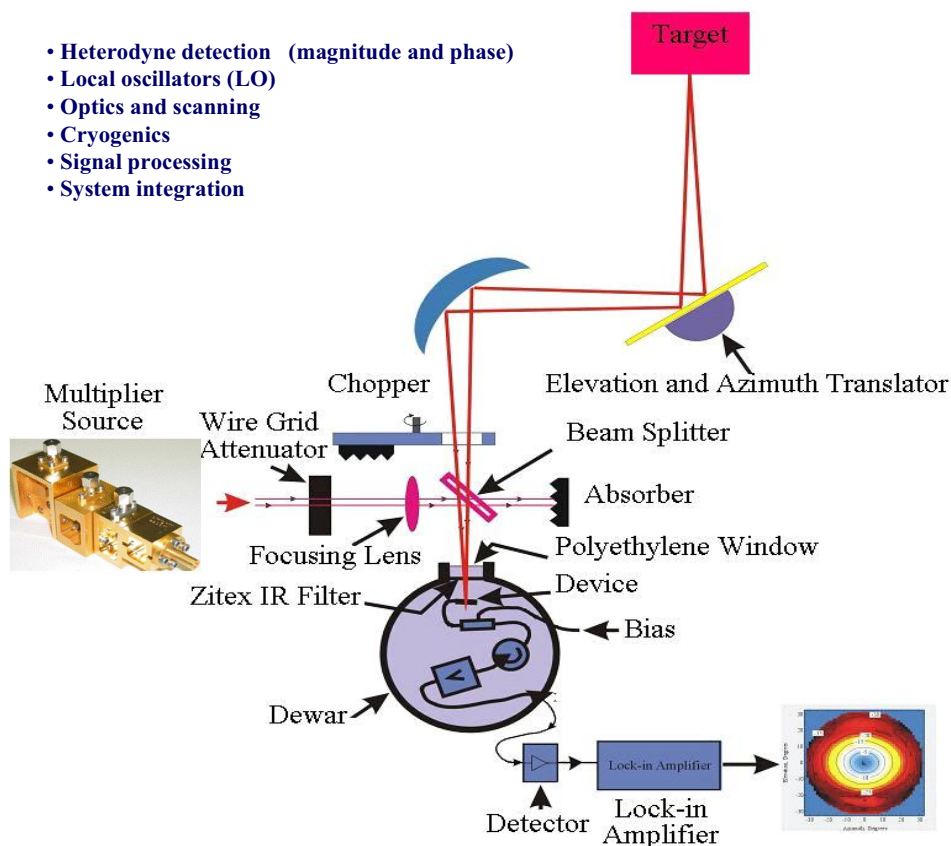
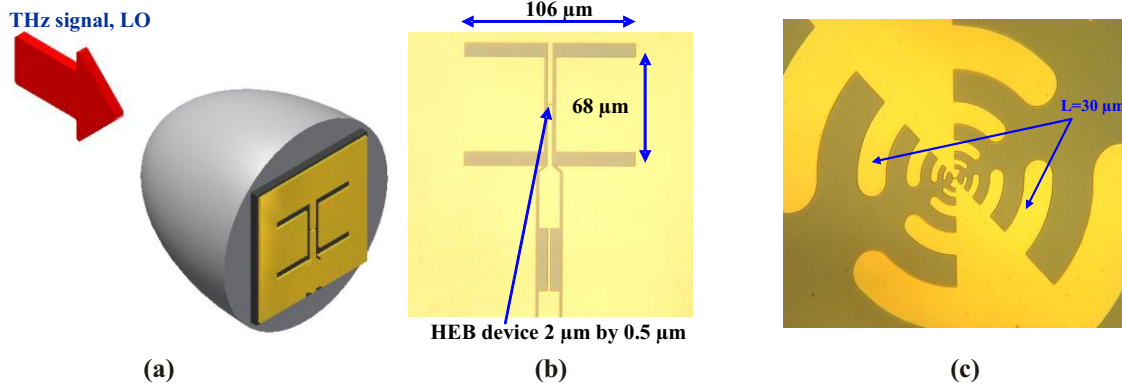


Figure 2: A schematic of a two-dimensional terahertz passive imaging system.



**Figure 3:** (a) a quasi-optical design illustration; (b) a photograph of the twin-slot antenna; (c) a photograph of the log-periodic antenna. The HEB devices in the centers of the antennas are too small to be seen.

aspect ratio. We also use the fact that its impedance at terahertz frequencies (well above the superconducting bandgap frequency) is real and has a value equal to its normal resistance just above the critical temperature. HEB devices are able to absorb the terahertz radiation up to the visible range due to the very short momentum scattering times. HEBs change their resistance as the quasi-particles are heated as a function of the incoming energy. These two properties are independent of the RF/LO frequencies. NbN HEBs have a thermal time constant that is determined by both the rate at which phonons are emitted by the electrons and the escape rate of the phonons from the NbN film to the substrate. For our devices, the resulting conversion gain bandwidth is about 3 to 3.5 GHz, while the receiver noise temperature bandwidth can be up to twice the gain bandwidth. An operating temperature range for the HEB devices of 4 K to about 6 K is an advantage compared to most other far-infrared (FIR) devices, which require cooling to sub-kelvin temperatures.

## 2.2 Quasi-optical coupling

In order to effectively couple the incoming radiations onto the HEB mixer, we have designed a quasi-optical system consisting of a silicon lens and a monolithic antenna centered at 850 GHz, as shown in Figure 3. The twin-slot antenna is patterned on a silicon substrate by use of an electron-beam metallization step followed by a lift-off step. The HEB device, made of an ultra-thin NbN film, with dimensions of 2  $\mu\text{m}$  (width)  $\times$  0.5  $\mu\text{m}$  (length), is located between the terminals of the twin-slot antenna. The twin-slot antenna has a highly symmetrical and linearly polarized radiation pattern and provides nearly perfect power coupling to the incident Gaussian beam [7]. The majority of HEB receivers now use quasi-optical coupling to the incoming radiation field by use of a combination of a dielectric lens and an integrated antenna (see Figure 3). We have employed three types of antennas: twin-slot antennas, which have a bandwidth of about 30 %, log-periodic antennas, which can be designed to have several octaves of bandwidth, depending on the number of teeth, and slot-ring antennas [8], which allow for a more efficient LO injection scheme. The terahertz signals couple to the device through an elliptical silicon lens (4 mm in diameter). The lens is a rotational ellipsoid that functions as an aperture antenna, and hence reshapes the far-field radiation pattern. By using a ray-tracing technique, the radiation from the twin slot antenna, placed at the second focus of the lens, becomes a plane wave in the aperture plane outside the lens. By considering the combination of the silicon lens and the twin-slot antenna, the far-field beam has a full-width half-power (FWHP) of about 3 degrees.

## 2.3 LO source

The practical available choices of LO sources at terahertz frequencies include far-infrared (FIR) lasers operating on a number of discrete spectral lines throughout the terahertz spectrum, and harmonic multiplier sources in the lower terahertz spectrum.

We have chosen a harmonic multiplier source as the LO because of its compact size and ease of use. A commercially available 850 GHz harmonic multiplier source [9] is employed as the LO signal. A phase-locked oscillator generates an output signal at 11.8 GHz. This signal is used to drive a multiplier chain, which is composed of one amplifier, two triplers, and three doublers. The entire chain produces a total frequency multiplication of 72 times, generating an output signal of 850 GHz. The terahertz signal injection is achieved by use of a WR 1.2 diagonal horn module assembled at the end of the multiplier chain. This particular harmonic multiplier source produces an output power of about 250  $\mu$ W. In order to combine the LO and the signal radiations, we employ a 25  $\mu$ m thick mylar beam splitter that reflects 28 % of the incoming LO radiation.

#### 2.4 Integrated receiver block

In a typical receiver system, the mixer and the LNA are assembled in separate blocks and connected by coaxial cables. An isolator is often included between the mixer and the LNA in order to minimize the standing wave between them. Although this configuration has been widely adopted in astrophysical receiver systems [2] [5], it does not meet the requirement for a compact multi-pixel FPA. Furthermore, the use of isolators limits the IF bandwidth to no more than an octave.

In order to eliminate the use of isolators, we have accomplished a design for integrating the HEB device and the MMIC LNA in the same block [10] (see Figure 4). A multi-section microstrip matching network is employed to achieve broadband coupling between the HEB and the MMIC LNA. The HEB device is located in close proximity to the MMIC chip, which is mounted in a narrow rectangular cavity for the purpose of eliminating possible amplifier oscillations. This particular MMIC LNA has been characterized against standards developed at the National Institute of Standards and Technology (NIST) and, by use of a recently developed measurement technique [11], exhibits noise performance of below 5.5 K from 1 GHz to 11 GHz. Figure 4 shows a photograph of the HEB/MMIC integrated mixer block. To couple the DC signal to the device and extract the IF signal from the device, we use a bias “tee” circuit that is built into the mixer block.

#### 2.5 Beam scan and data acquisition

A scanning scheme was designed to record the image of the target by means of a line-by-line sweep, often called a raster scan. Each line of the scan is divided into a number of pixels. The number of pixels and the distance between pixels can be adjusted according to the desired resolution and the size of the target. The total wait period at each pixel is based on the lock-in integra-

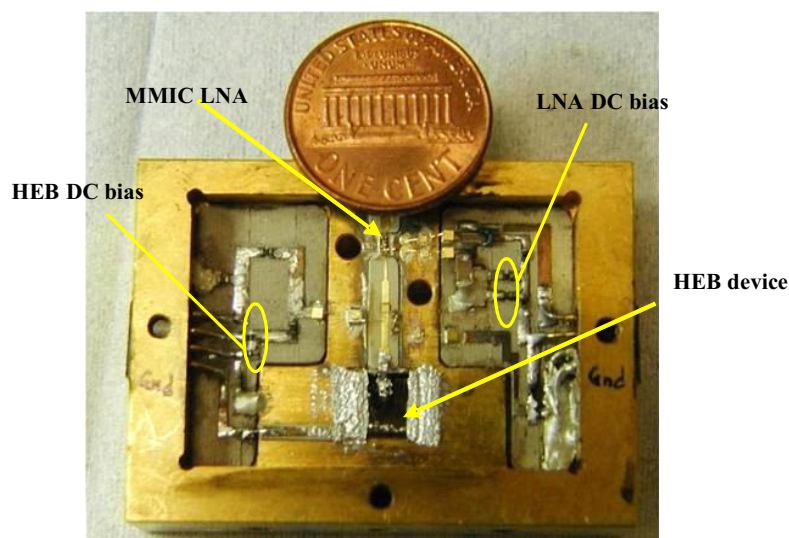


Figure 4: An integrated mixer block housing an HEB device and an MMIC LNA.

tion time constant. In order to achieve fast scanning and stability of signal, the wait period is made about three times longer than the lock-in time constant. An automated motion controller, which also functions as a DAQ system, is used to drive the translator and collect the data in real-time. The motion controller provides a 0.001 degree angular resolution and can gather data with 14 bit accuracy ( $\pm 600 \mu\text{V}$  on a  $\pm 10 \text{ V}$  scale) at rates up to 10 kHz. The motion controller has a built-in microprocessor and is capable of communicating with a host computer via Ethernet protocol.

### 3. HETERODYNE AND DIRECT DETECTORS COMPARISON

The choice between an imager based on heterodyne detectors or direct detectors is not an easy one. Depending on the application, a designer can tailor the instrument to perform better by understanding the similarities and differences of the two types of detectors. Some applications dictate the type of detector to be used. In order to promote understanding of the figures of merit of both detector technologies, a direct comparison is summarized in TABLE I. In general, in order to resolve magnitude and phase of a signal, a heterodyne detector should be chosen. A heterodyne detection system down-converts the signal into an intermediate frequency (IF) and requires a local oscillator source. For higher spectral resolution, heterodyne detector technology is preferable. The figure of merit for the sensitivity of direct detectors is the noise equivalent power (NEP), whereas noise temperature is used for heterodyne detectors. The distinction between system noise temperature and receiver noise temperature is that the former includes the noise from the input source (ideally the vacuum fluctuations), whereas the latter includes the noise generated in the receiver only. Obviously, it is the system noise temperature that determines the sen-

TABLE I  
SUMMARY OF NOISE FIGURES OF MERIT

Heterodyne Detector	Direct Detector
<ul style="list-style-type: none"> <li>• <i>HEB (Hot Electron Bolometer) Mixer:</i> DSB Noise temp. <math>\sim 900 \text{ K}</math> (at 4-6 K) Bandwidth 4 GHz <math>\Delta T_{RMS} \geq 2T_{sys} / \sqrt{B\tau} = 90 \text{ mK}</math> in 0.1 sec and 28 mK in 1 sec</li> <li>• <i>SBD (Schottky Barrier Diode) Mixer:</i> DSB Noise temp. <math>\sim 3,600 \text{ K}</math> (at room temp.) Bandwidth 12 GHz <math>\Delta T_{RMS} \geq 2T_{sys} / \sqrt{B\tau} = 208 \text{ mK}</math> in 0.1 sec</li> <li>• <i>HEB and SBD are quite similar in terms of sensitivity.</i> <math>NEP_{HEB} (1 \text{ sec}) = k B \Delta T_{RMS} = 1.6 \cdot 10^{-15} \text{ W} / \sqrt{\text{Hz}}</math> <math>NE\Delta T_{HEB} (1 \text{ sec}) = \Delta T_{RMS} = 28 \text{ mK}</math> <math>NE\Delta T_{HEB} (0.03 \text{ sec}) = \Delta T_{RMS} = 162 \text{ mK}</math></li> </ul>	<ul style="list-style-type: none"> <li>• <i>Nb direct detector [12]:</i> Frequency about 100 GHz: Active system (IMPATT at 1W peak) <math>NEP_{Nb} (1 \text{ sec}) = 5 \cdot 10^{-11} \text{ W} / \sqrt{\text{Hz}}</math> at room temp. <b>Improved <math>NEP_{Nb} (1 \text{ sec}) = 5 \cdot 10^{-12} \text{ W} / \sqrt{\text{Hz}}</math> at room temp.</b> Frequency about 100-1000 GHz: <math>NEP_{Nb} (1 \text{ sec}) = 4 \cdot 10^{-13} \text{ W} / \sqrt{\text{Hz}}</math> at 4 K [13]</li> <li>• <math>NE\Delta T_{Nb} = NEP_{Nb} / (k B)</math> in 1 sec integration time Assume spectral bandwidth of 10 GHz <b>For <math>NEP_{Nb} = 4 \cdot 10^{-13} \text{ W} / \sqrt{\text{Hz}}</math>, <math>NE\Delta T_{Nb} (1 \text{ sec}) = 2.9 \text{ K}</math></b> <math>NE\Delta T_{Nb} (0.03 \text{ sec}) = 16.7 \text{ K}</math></li> </ul>

sitivity of a heterodyne detector system in an imaging application. In order to compare the sensitivity of a heterodyne detector with that of a direct detector used in an active imaging system (the target is illuminated), the noise temperature of the heterodyne detector has to be converted to noise equivalent power (see TABLE I). Detectors for passive systems are characterized by their noise equivalent difference in temperature (NE $\Delta$ T). TABLE I compares these figures of merit (NEP, NE $\Delta$ T) for existing detector technologies. In general, cooling a detector improves its sensitivity (i.e., lowers its intrinsic noise). Direct detectors made of Nb show, when cooled to 4 K, an improvement of about three orders of magnitude in their NEP performance [13]. We must also distinguish between “electrical” and “optical” NEP values. Electrical NEP values (NEP<sub>e</sub>) are deduced from the IV-curve and the measured output noise, while optical NEP values are deduced from actual “optical” measurements on targets switched between known temperatures. To evaluate the system performance, the optical NEP (NEP<sub>opt</sub>) should be used. The best performance reported for a direct detector at 4 K is for a thermally-isolated Nb thin bridge [13]. It was measured to yield  $NEP_{opt}(1\text{ sec}) = 4 \cdot 10^{-13} \text{ W}/\sqrt{\text{Hz}}$  when the detector senses a very wide RF frequency range from 0.1 to 1.0 THz. Such a wide frequency range would not be useful in a terahertz imaging system requiring high spatial resolution; for example, the beamwidth sensed by the optics would vary by a factor of ten over the frequency range (determined by the aperture size in wavelengths). In addition, for performing spectroscopy with high spectral resolution, a drastic narrowing of the bandwidth is required. The NEP figure for the HEB receiver given in TABLE I ( $1.6 \cdot 10^{-15} \text{ W}/\sqrt{\text{Hz}}$ ) is at least two orders of magnitude better than that of the best direct detector. That comparison applies to an active imaging system. For passive imaging systems, we should instead compare the NE $\Delta$ T of an HEB with the above Nb direct detector [13]. For a coarse spectral resolution of 10 GHz, the Nb direct detector [13] has an NE $\Delta$ T of 16.7 K at an integration time of 30 ms, whereas the HEB receiver system quoted in TABLE I has NE $\Delta$ T = 162 mK. We will discuss the actual performance of our present passive imaging system later on in this paper, but mention already that we are approaching the performance of the optimum HEB system. Nb HEB detectors, with the sensitivity of those in [13], have not been demonstrated at higher frequencies than 1 THz, whereas HEB detectors can be used over the entire terahertz range with similar performance. One clear advantage of the direct detectors used in imaging is the lack of LO source requirement.

#### 4. IMAGING RESULTS AND DISCUSSION

Figure 5 shows our passive terahertz imaging system. The LO and signal beams are marked with blue and green lines, respectively. The imager footprint and the size of the optical mirrors can be kept small due to the short wavelength at 850 GHz (352  $\mu$ m). We use a special absorber material [14] (the orange absorbing material in Figure 5) designed to work at terahertz frequencies. The specular reflectance of this absorber was measured recently as a function of frequency (see Figure 6) [15]. The HEB receiver in our imaging system has a noise temperature of 1800 K. This is not the most sensitive HEB mixer we have produced [1]. The integration time constant on the lock-in amplifier was 300 ms, which integrates 60 periods of the chopping frequency (200 Hz). The IF bandpass filter, with a center frequency of 2.35 GHz and a bandwidth of 2.3 GHz, ensures the best overall performance in terms of low noise and widest bandwidth. We can enhance the spatial resolution of the image by minimizing the beam waist on the target. In our case, we had a beam waist of about 3.6 mm. The DAQ system allows for three periods of the lock-in amplifier time constant (1 s) at each pixel, resulting in about 30 minutes to complete a scan of a 40 by 40 pixel image. For our imager, the RMS fluctuation in the measured radiation temperature can be obtained according to the radiometer formula:

$$\Delta T_{RMS} = \frac{2T_{SYS}}{\sqrt{B_{eff}\tau}} = \frac{2 \times (1800 + 300)}{\sqrt{2.3 \times 10^9 \times 0.3}} = 160 \text{ mK}, \quad (1)$$

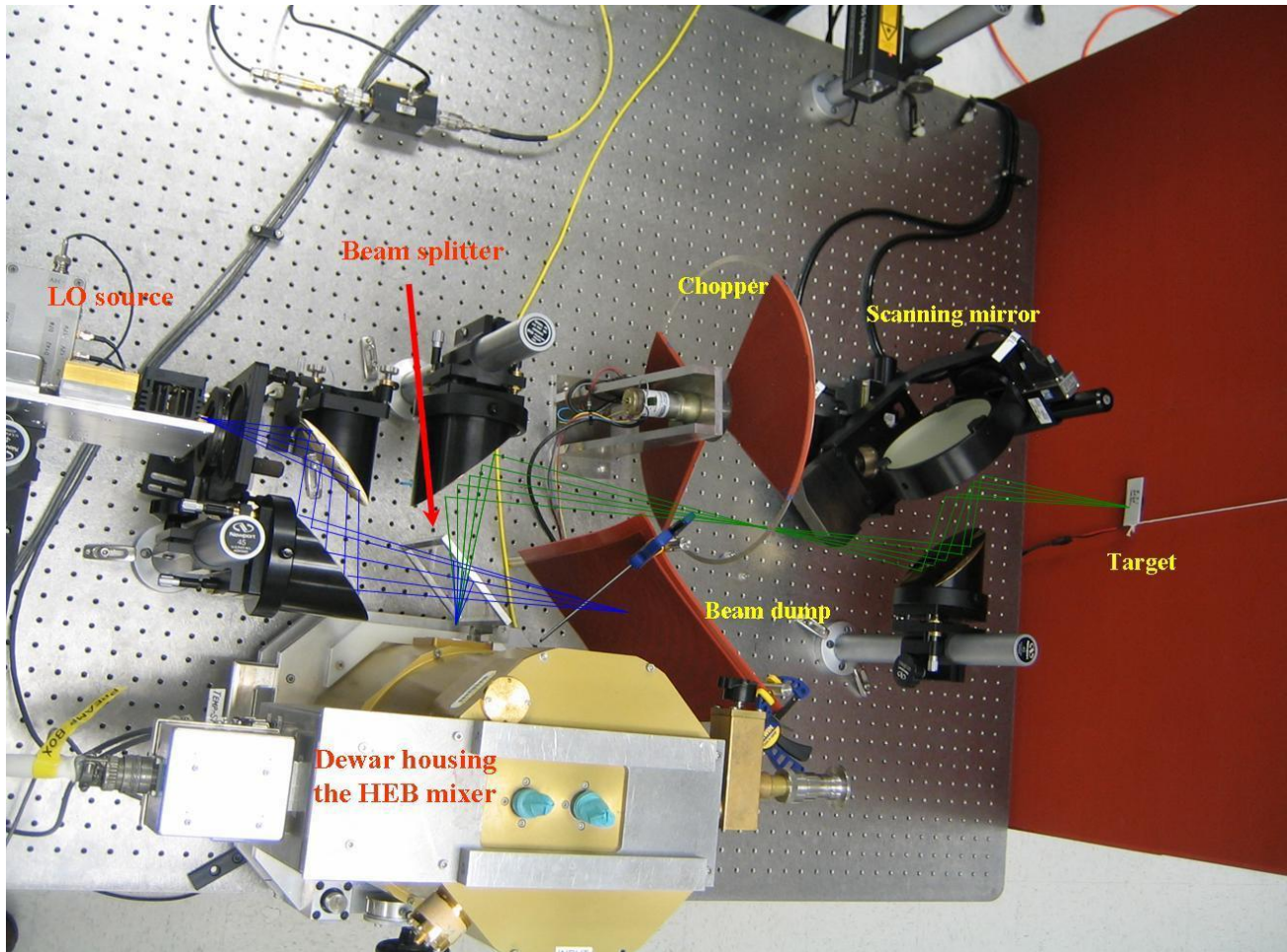


**Figure 5: A photograph of the 2D passive terahertz imager operating at 850 GHz.**

where  $T_{\text{sys}}$  is the system noise temperature,  $B_{\text{eff}}$  is the receiver bandwidth, and  $\tau$  is the integration time. In our case, the imaging system can theoretically resolve a temperature difference as small as 160 mK. The system temperature can be decreased to 1000 K with optimum HEB detectors, while the bandwidth may be increased to at least 3 GHz, resulting in  $\text{NE}\Delta T = 37$  mK, normalized to a 1 s integration time. For a typical video imaging rate, the integration time would be 30 ms and  $\text{NE}\Delta T = 210$  mK. The best published results for a direct detector translates to  $\text{NE}\Delta T$  of about 1 K as discussed earlier [13]. Presently, heterodyne systems are more sensitive by a factor of five or better. So far, we note that the data for the Nb direct detector in [13] are only for a single element, not an imaging system.

Figure 7 shows an example of two room-temperature objects forming a cross suspended over an absorber immersed in liquid nitrogen. The temperature difference (of about 200 K) can be clearly distinguished by the color contrast. In order to characterize the thermal resolution of the imaging system, we used a target made of a resistor coil in front of a room-temperature absorber (see Figure 8). The temperature difference between the resistor coil and the absorber can be adjusted by changing the voltage across the resistor. Images at 850 GHz were taken for two different temperature differences: 3 K and 1 K. The hot spot corresponding to the warmer coil for the 3 K temperature difference is clearly observed from Figure 8(b). We can estimate an actual  $\text{NE}\Delta T = 430$  mK for the present system.



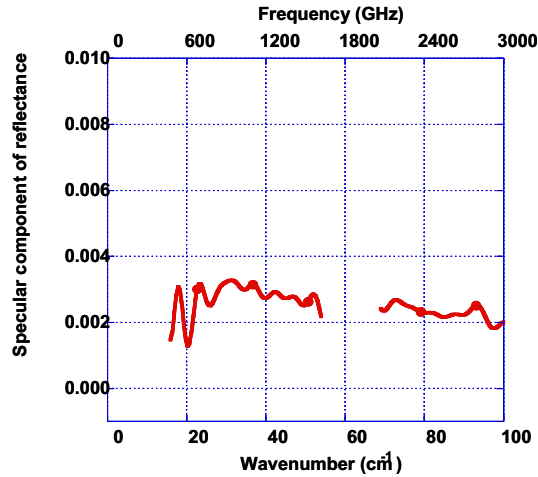


Figure 6: Specular reflectance measurement as a function of frequency of the terahertz absorber used in the imager [15].

## 5. SUMMARY AND FUTURE WORK

We have developed a two-dimensional passive terahertz imaging system operating at 850 GHz based on HEB technology. The demonstrated thermal resolution is about 430 mK. By reducing the noise temperature of the HEB device and cleaning some of the system noise, a substantial improvement in total imager sensitivity can be achieved. The detection speed can be increased by employing a faster chopper. The next step for increasing system speed will be to use an FPA. A prototype FPA containing three elements based on HEB mixers and MMIC LNAs has already been demonstrated [10]. Figure 9 shows a conceptual architecture for future large FPAs using multiple HEB detectors. This design can be extended to a large number of elements. Initially, the architecture shown here will be implemented for a small number of elements. The lenses and the HEB

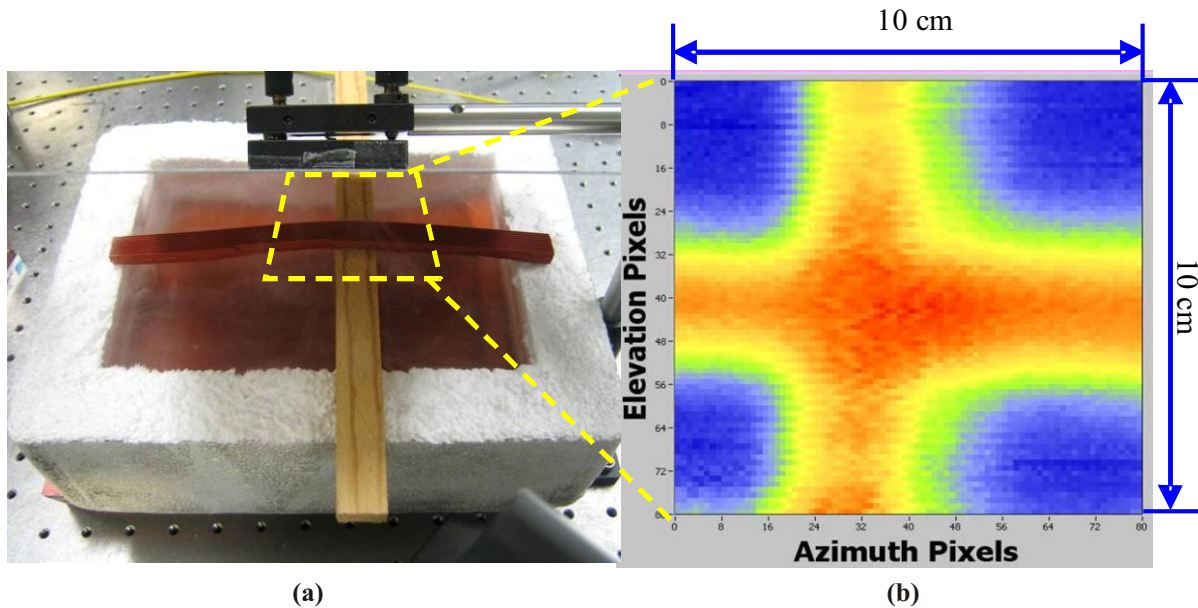
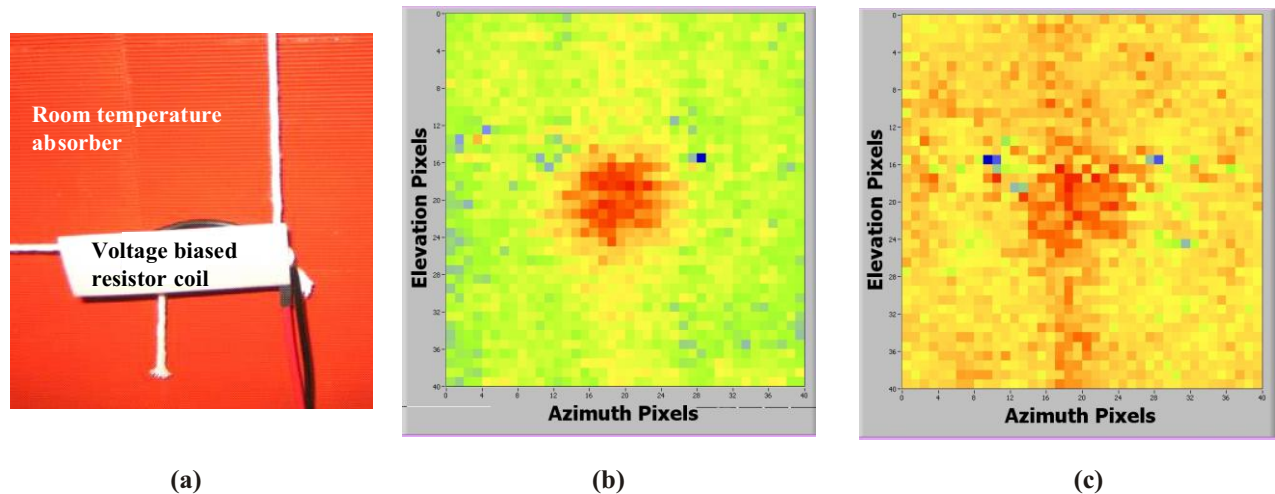


Figure 7: (a) A photograph and (b) a 850 GHz image of two room temperature objects suspended over an absorber immersed in liquid nitrogen. Red corresponds to warm temperatures and blue corresponds to cold temperatures (~200 K difference).



**Figure 8: (a) photograph of the resistor coil and the absorber; (b) image of 3 K difference; (c) image of 1 K difference.**

devices will be arranged in a fly's eye configuration. Such a configuration can produce an angular resolution slightly larger than one diffraction-limited beamwidth (FWHM). The MMIC IF amplifiers will be assembled on a separate substrate and contacted through via holes. As an alternative, this substrate will be attached to a cooling stage at 15-20 K, in order to improve the cooling requirements of the array. The amplifiers would then be contacted through coplanar waveguide or microstrip lines on flexible Kapton ribbons. We expect that this new architecture, combined with MEMS micro-cryocooler technology, currently under development, will potentially be able to produce an extremely compact system for mobile terahertz imagers with video-rate speeds. Potential applications for these receivers range from medical diagnostics to security surveillance.

## REFERENCES

1. E. Gerecht, et al., "NbN Hot Electron Bolometric Mixers, a New Technology for Low-Noise THz Receivers," IEEE Trans. Microw. Theory Tech., vol. 47, no. 12, pp. 2519–2527, Dec. 1999.
2. E. Gerecht, et al., "Deployment of TREND – A Low Noise Receiver User Instrument at 1.25 THz to 1.5 THz for AST/RO at the South Pole". 14<sup>th</sup> Intern. Symp. Space THz Technology, Tucson, Az, Apr. 2003.
3. J. Kawamura et al., "First Light with an 800 GHz Phonon-Cooled HEB Mixer Receiver," p. 35-43, 9<sup>th</sup> ISSTT, (1998).
4. S. Radford, "CO(9-8) in Orion," 14th Intern. Symp. Space THz Technology, Tuscon, AZ, (April 2003).
5. S. Cherednichenko, et al., "1.6 THz heterodyne receiver for the far infrared space telescope." Physica C, vol. 372–376, pp. 427–431, 2002.
6. D. Gu, E. Gerecht, F. Rodriguez-Morales, and S. Yngvesson, "Two-Dimensional Terahertz Imaging System Using Hot Electron Bolometer Technology", 17th Intern. Symp. Space THz Technol., Paris, France, April 10-12, 2006.
7. D. F. Filipovic, S. S. Gearhart, and G. M. Rebeiz, "Double-Slot Antenna on Extended Hemispherical and Elliptical Silicon Dielectric Lenses," IEEE Trans. Microw. Theory Tech., vol. 41, no. 10, pp. 1738–1749, Oct. 1993.
8. E. Gerecht, D. Gu, X. Zhao, J. Nicholson, F. Rodriguez- Morales, S. Yngvesson, "Development of NbN Terahertz HEB Mixers Coupled Through Slot Ring Antennas", 15th Intern. Symp. Space THz Technol., Northampton, MA, April 27-29, 2004.
9. Virginia Diodes, Inc, <http://www.virginiadiodes.com/multipliers.htm>

10. F. Rodriguez-Morales, S. Yngvesson, R. Zannoni, E. Gerecht, D. Gu, N. Wadefalk, and J. Nicholson, "Development of Integrated HEB/MMIC Receivers for Near-Range Terahertz Imaging," IEEE Trans. Microw. Theory Tech. vol. 54, no. 6, Jun. 2006.
11. J. Randa, E. Gerecht, D. Gu, and R. Billinger, "Precision Measurement Method for Cryogenic Amplifier Noise Temperatures Below 5 K," IEEE Trans. Microw. Theory Tech., vol. 54, no. 3, pp. 1180–1189, Mar. 2006.
12. S. Nolen, J.A. Koch, N.G. Paulter, C.D. Reintsema, and E.N. Grossman, "Antenna-Coupled Bolometers for Millimeter-Wave Imaging Arrays," Proc. SPIE 3795 (1999).
13. A. Luukanen, et al., "An Ultra-Low Noise Superconducting Antenna-Coupled Microbolometer With a Room-Temperature Read-Out," IEEE Microw. and Wireless Compon. Lett., Vol 16, No. 8, August 2006.
14. Specialized terahertz absorber from the University of Mass. at Lowell.
15. Measurements performed by Simon Kaplan at NIST/Gaithersburg.

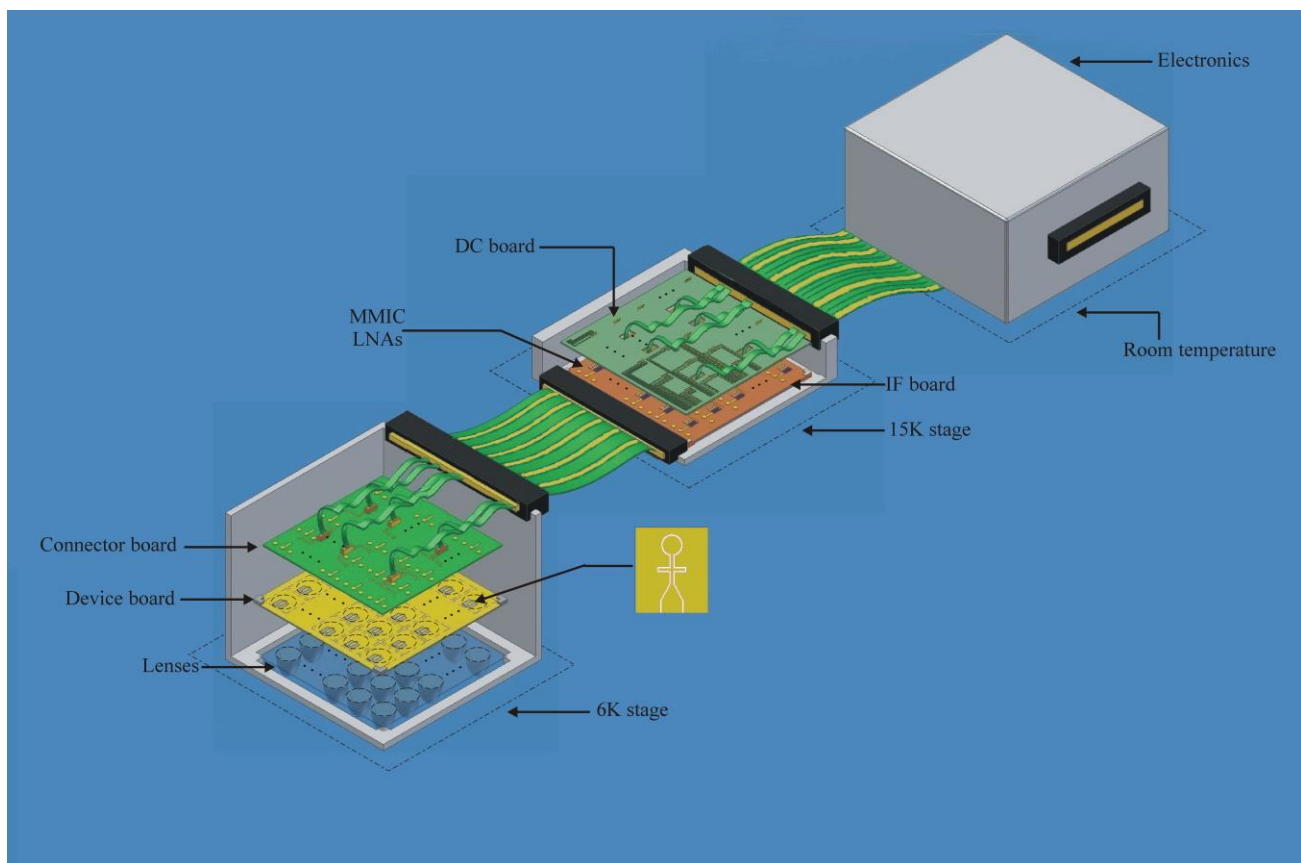


**Figure 9: A conceptual configuration for a terahertz heterodyne focal plane array with HEB devices.**